

Chapter 5: New Methodology for Estimating Aerosol

This chapter presents a technique developed in this study for analysing urban aerosol. A mathematical model is developed for determining the aerosol optical depth from the strong gaseous absorption due to atmospheric oxygen at around 760 nm. The model is validated using high spectral resolution ground-based spectroradiometric data and Hyperion hyperspectral images.

5.1. Purpose of the Work

Along with the increase in CO₂, aerosol loading to the urban atmosphere is a sign of human activity. As a result, the current effort focuses on assessing urban aerosol using hyperspectral remote sensing and developing an independent approach for that purpose.

As discussed in Chapter 2, the aerosol optical depth is often measured using radiation with lower atmospheric attenuation. The current paper takes a new approach to the phenomenon, proposing a technique for determining aerosol optical depth based on the significant gaseous absorption of air oxygen at about 760 nm, known as the O₂-A band. Ground-measured spectroradiometric data and Hyperion image analysis are used to validate the approach. It varies from prior approaches in the following ways (Dubuisson et al., 2009).

- It utilises two non-absorbing bands on either side of the absorbing band, rather than one.
- There is no requirement for a reference parameter such as top-of-atmosphere reflectance.
- There are several benefits of using the O₂-A band. Its position on the radiance spectral curve is sharp and prominent, hence precisely detectable by a hyperspectral instrument. Also, the location of the absorption band is universal and stable over a wide range of atmospheric conditions. Also, the O₂-A absorption can be achieved with any radiation, solar or man-made, irrespective of the radiation source or its intensity.

The current method is expected to be appropriate to the aerosol assessment at different places under the same meteorological conditions. Its limitation is that it cannot

discriminate between different types of aerosols, such as size distribution. However, that is outside the scope of this document. This work is concerned with the gross geographic distribution of aerosols, and the current approach is capable of doing so.

5.2. Methodology and Data

5.2.1. Developing the Optical Depth Model

The radiance (L_i) transmitted through an atmospheric column is generally quantified in terms of the Beer-Bouguer-Lambert law for a specific wavelength. However, at the wavelengths of strong gaseous absorption, such as that of the O₂-A band, the above formulation does not hold. The present work formulates the absorption process under the gaseous absorption condition in the following generalized way.

The *measured radiance* (L_m) at the sensor for any arbitrary wavelength depends on the following three quantities:

- the *source radiance* (L_s), which is either emitted from a source or reflected from an object surface,
- the gaseous absorption, if any, through the atmospheric path and
- the radiance gained by aerosol scattering and Rayleigh scattering over the traversing path, hence termed as *path radiance* (L_p).

The at-sensor radiance is the algebraic sum of the above three parameters. Since the Rayleigh scattering is very low in the NIR wavelength range (750–775 nm) including the O₂-A band of present interest, only the aerosol contribution is considered here. There is another significant absorbing agent that is the water vapour. However, it has specific absorption bands about 710–740 nm and 800–840 nm that are beyond the range of the present concern. So, the water vapour absorption is supposed to cast a uniform effect all the way. Considering these all, the observed radiance inside the O₂-A band at the wavelength of maximum absorption may be represented as

$$L_{ma} = TL_s + L_{pa} \quad (5.1)$$

The atmospheric transmittance in this band is denoted by T . The subscript ‘ a ’ stands for ‘absorption’. The measured radiance for any other non-absorbing wavelength outside of this band is

$$L_m = L_s + L_p \quad (5.2)$$

Because there is no particular gaseous absorption, T becomes unity (100%). If L_s becomes insignificant, the measured radiance (L_m) is basically equal to the path radiance (L_p). Eqs. (5.1) and (5.2) are used to calculate the transmittance in the O₂-A band. Eq. (5.2) can be generalised if several reference wavelengths are used instead of a single wavelength as

$$T = \frac{L_{ma} - L_{pa}}{\sum_i w_i (L_{mi} - L_{pi})} \quad (5.3)$$

For each i -th band, the relative weight (w_i) for each reference pair of wavelength (λ_1 and λ_2) on either side of the absorbing wavelength (λ_a) is given by

$$w_1 = \frac{\lambda_2 - \lambda_a}{\lambda_2 - \lambda_1} \quad \text{and} \quad w_2 = \frac{\lambda_a - \lambda_1}{\lambda_2 - \lambda_1} \quad (5.4)$$

The path radiance (L_{pi}) for any i -th reference band outside the O₂-A band may not be the same as the path radiance (L_{pa}) within the absorbing O₂-A band but one can be expressed as a fraction or multiple of the other so that

$$L_{pi} = q_i L_{pa} \quad (5.5)$$

The parameter q_i in Eq. (5.5) stands for a constant of proportionality for i -th band. Eq. (5.5) is substituted to Eq. (5.3) and rearranged to derive the expression for a relative optical depth as

$$T_0 = T + \frac{L_{pa}}{\sum_i w_i L_{mi}} (1 - T \sum_i w_i q_i) \quad (5.6)$$

In Eq. (5.6), $T_0 = \frac{L_{ma}}{\sum_i w_i L_{mi}}$ represents the relative optical depth at the O₂-A band

in presence of aerosols. The significance is that this quantity is experimentally measurable.

Eq. (5.6) accounts for both oxygen absorption and aerosol scattering. When there is no aerosol, one can put $L_{pa} = 0$ in Eq. (5.6) to obtain $T_0 = T$. The physical meaning is that the relative optical depth (T_0) at O₂-A band becomes equivalent to the transmittance solely due to gaseous absorption when there is no aerosol. The term ‘relative’ is used because it refers to how the absorption is evaluated in relation to the measured spectral data. The above formulation has the advantage that it is based only on simultaneously measured experimental quantities and does not require any absolute reference value, such as the extra-terrestrial radiation for the calculation.

5.2.2. Ground measurements and Image analysis

The field work for procuring the incident solar irradiance spectra at different atmospheric conditions was conducted at a densely populated urban area of Kolkata (22°39′19.24" N, 88°23′00.33" E). The ground based high resolution spectroradiometric measurements were carried out with Analytical Spectral Devices FieldSpec spectroradiometer having spectral resolution of 1.4 nm throughout the ultraviolet-visible-near-infrared (UV-vis-NIR) ranges of wavelength. The instrument equipped with a remote cosine receptor on a 25° field-of-view fibre was kept at the same vertically upward-facing position and at the same location in open air for different solar elevations. The measurements were recorded around solar noon. The same regulations were maintained carefully for different days, seasons and meteorological conditions.

Hyperion hyperspectral pictures for Kolkata and the surrounding region (centred about 22°35' N, 88°24' E) were obtained from the US Geological Survey website (<https://www.usgs.gov>) to compare the measured data with those produced from satellite images. The images were analysed with ENVI 4.7 image processing software. The raw

digital number (DN) values for all pixels for each of the fifty VNIR waveband channels (No. 8 to 57) were converted to the corresponding reflectance (R) values by the conventional procedure of

$$R = \frac{\pi L_{\lambda} d^2}{ESUN_{\lambda} \cos \theta} \quad (5.7)$$

Where

$L_{\lambda} \equiv \text{DN}/40$ is the radiance ($\text{Wm}^{-2}\text{sr}^{-1}\mu\text{m}^{-1}$) as function of wavelength

$d \equiv$ earth-sun distance in astronomical units

$ESUN_{\lambda} \equiv$ Hyperion mean solar exoatmospheric irradiance ($\text{Wm}^{-2}\mu\text{m}^{-1}$) as function of wavelength and

$\theta \equiv$ solar zenith angle

5.3. Results on Optical Depth

Figure 5.1 shows the theoretical variation of relative optical depth generated by Eq. (5.6) adjusting the q_i and L_{pa} parameters. The different extents of aerosol path radiance are generated as percentages of the measured radiance (L_{ma}) values within the O₂-A band, the ‘no aerosol’ condition being represented by zero percent. To understand the extreme conditions, some highly exaggerated q_i values are also used and it is interesting to note that the transmittance does not deviate by more than 17 percent even for the worst case. Thus, it is not unreasonable to infer that $q_1 = q_2 = 1$ denotes the same path radiance over the wavelength range under consideration.

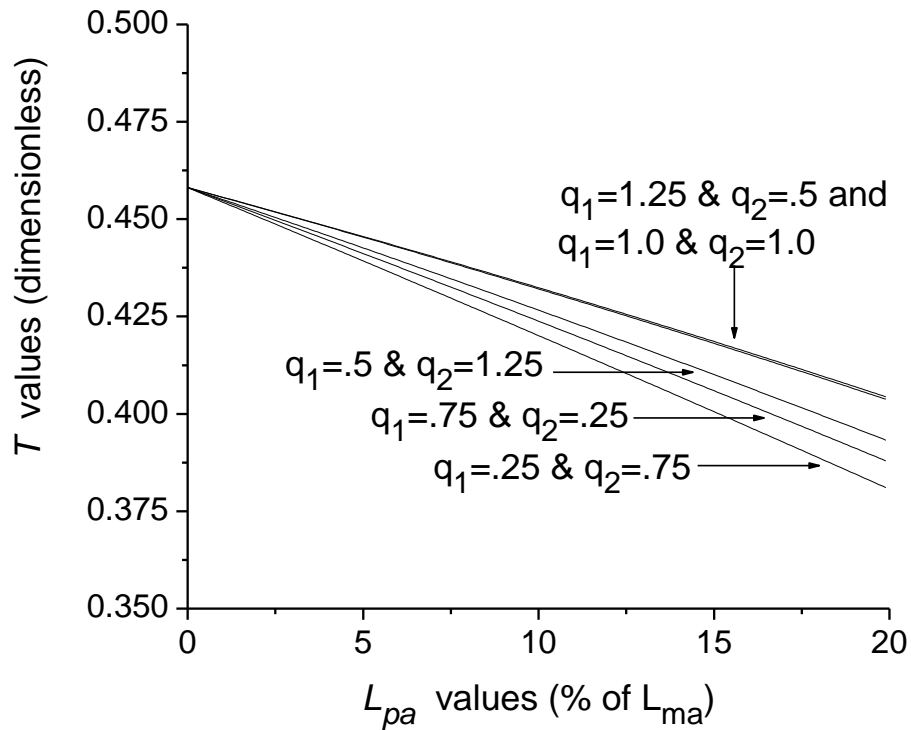


Figure 5. 1. Relative optical depth generated with Eq. (5.6) and its change with various extents of aerosol path radiance (L_{pa}). The relative contributions of two reference wavelengths (756 nm and 772 nm) to path radiance are accounted for by q_1 and q_2 , respectively.

The O₂-A absorption depths were measured both at full-sun and under cloudy condition and also at different seasons, such as summer and winter. It was verified that the extent of change in the absorption depth caused by aerosols estimated above was of the same scale as that caused by other atmospheric parameters. It implies that the aerosol-related change assessed by the present method should be compared between two identical atmospheric conditions only, such as those under the same solar elevation or with comparable intensity of solar radiation.

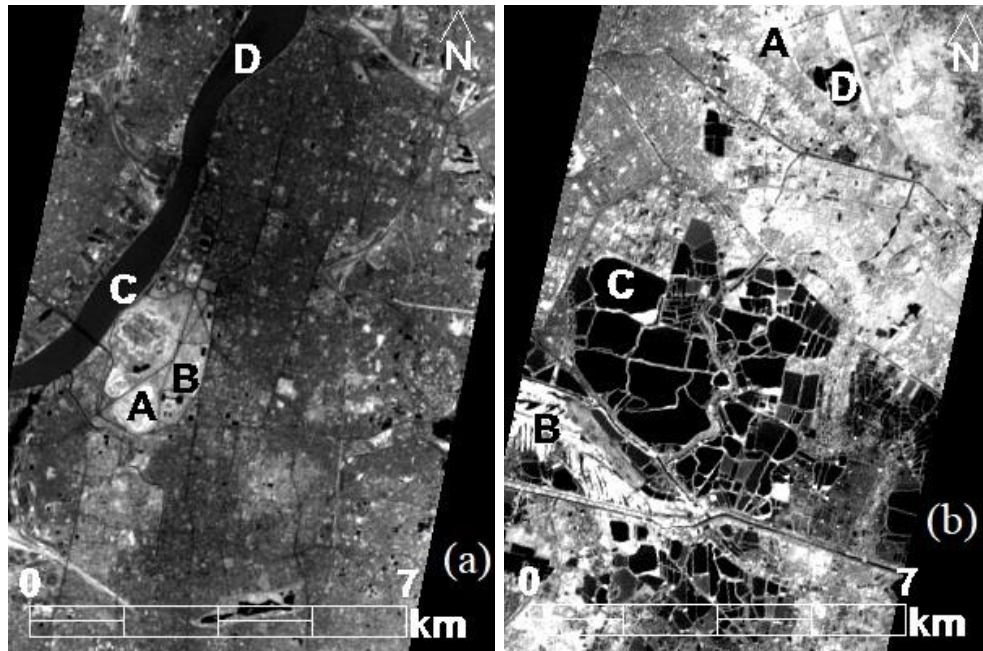


Figure 5. 2. Hyperion images of Kolkata dated (a) July 27, 2002 and (b) January 6, 2010. The vegetated regions are denoted by 'A' and 'B' and waterbodies are denoted by 'C' and 'D'.

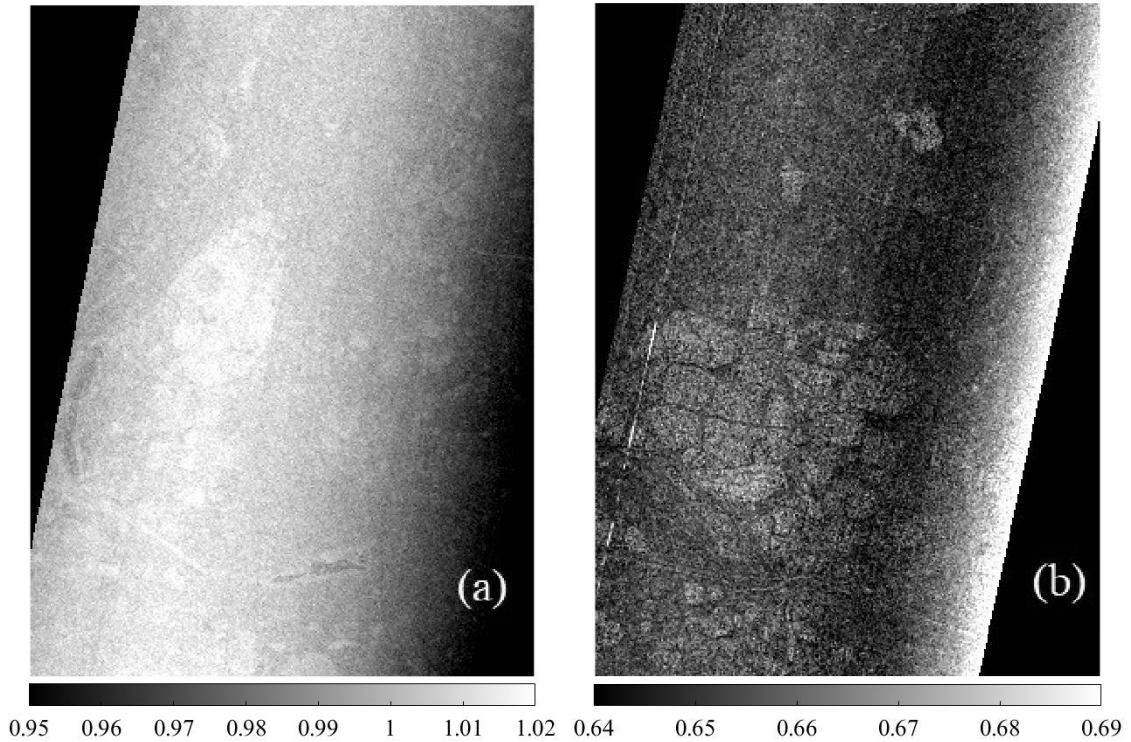


Figure 5. 3. Spatial variation of relative optical depth [Eq. (5.6)] determined for: (a) Figure 5.2(a) 0.95 to 1.02 and (b) Figure 5.2(b) 0.64 to 0.69. The O_2 -A band is band-41 (762.6 nm) and the two reference wavebands on either sides are band-40 (752.4 nm) and band-42 (772.8 nm).

Figures 5.2(a) and 5.2(b) show two Hyperion images of urban areas of Kolkata at two different periods. The region of Figure 5.2(b) is of less urban congestion than that of Figure 5.2(a). The common features are that the areas of the image consist of populated urban region with a river running beside it. Regions like ‘A’ and ‘B’ represent isolated vegetated lands within the city and regions like ‘C’ and ‘D’ indicate river and inland waterbody. Figures 5.3(a) and 5.3(b) display the corresponding spatial variations of relative optical depth (T_o) using Eq. (5.6) for these two images. The absorption and reference bands are mentioned in the figure caption. The optical depth for Figure 5.3(a) varies from 0.95 to 1.02 and that of Figure 5.3(b) ranges from 0.64 to 0.69. It is indicated that the more populated region corresponds to larger aerosol density, hence larger optical depth.

5.4. Inferences

The current study demonstrates that the influence of atmospheric aerosol can be quantified in terms of a relative optical depth detected at the strong gaseous absorption band of atmospheric oxygen at around 760 nm. Two non-absorbing wavebands are used as reference for determining the optical depth. The significance of this method is that the assessment is done purely from the measured spectral without using any additional parameter, such as the extra-terrestrial radiation. The technique is validated with ground-based hyperspectral solar irradiance measurements and the hyperspectral radiance data derived from Hyperion images. The technique is expected to be suitable for estimating the spatial variation of aerosol over the regions under similar atmospheric conditions.

Chapter References

Dubuisson, P., Frouin, R., Dessailly, D., Duforêt, L., Léon, J., Voss, K., & Antoine, D. (2009). Estimating the altitude of aerosol plumes over the ocean from reflectance ratio measurements in the O₂ A-band. *Remote Sensing of Environment*, 113(9), 1899-1911. doi: 10.1016/j.rse.2009.04.018